Human Molecular Genetics, 2009, Vol. 18, No. 23 ***4590–4602***
doi:10.1093/hmg/ddp426
Advance Access published on September 9, 2009

CDKL5 influences RNA splicing activity by its association to the nuclear speckle molecular machinery

Sara Ricciardi[1,2], Charlotte Kilstrup-Nielsen[1,3], Thierry Bienvenu[4], Aurélia Jacquette[5], Nicoletta Landsberger[1,3] and Vania Broccoli[1,2,*]

[1]Division of Neuroscience, San Raffaele Rett Research Center and [2]Stem Cells and Neurogenesis Unit, Division of Neuroscience, San Raffaele Scientific Institute, Milan 20132, Italy, [3]Department of Structural and Functional Biology, University of Insubria, Busto Arsizio, VA, Italy, [4]Laboratoire de Génétique et de Physiopathologie des Maladies Neuro-développementales, Université Paris Descartes, Institut Cochin, CNRS (UMR 8104), Inserm U567, 24 rue du Faubourg Saint Jacques, Paris 75014, France and [5]Service de Génétique Médicale, AP-HP, Hôpital Pitié-Salpétrière, 47-83, Boulevard de l'Hôpital 75651, Paris Cedex 13, France

Received July 1, 2009; Revised and Accepted September 3, 2009

Mutations in the human X-linked cyclin-dependent kinase-like 5 (*CDKL5*) gene have been shown to cause severe neurodevelopmental disorders including infantile spasms, encephalopathy, West-syndrome and an early-onset variant of Rett syndrome. CDKL5 is a serine/threonine kinase whose involvement in Rett syndrome can be inferred by its ability to directly bind and mediate phosphorylation of MeCP2. However, it remains to be elucidated how CDKL5 exerts its function. Here, we report that CDKL5 localizes to specific nuclear foci referred to as nuclear speckles in both cell lines and tissues. These sub-nuclear structures are traditionally considered as storage/modification sites of pre-mRNA splicing factors. Interestingly, we provide evidence that CDKL5 regulates the dynamic behaviour of nuclear speckles. Indeed, CDKL5 overexpression leads to nuclear speckle disassembly, and this event is strictly dependent on its kinase activity. Conversely, its down-regulation affects nuclear speckle morphology leading to abnormally large and uneven speckles. Similar results were obtained for primary adult fibroblasts isolated from *CDKL5*-mutated patients. Altogether, these findings indicate that CDKL5 controls nuclear speckle morphology probably by regulating the phosphorylation state of splicing regulatory proteins. Nuclear speckles are dynamic sites that can continuously supply splicing factors to active transcription sites, where splicing occurs. Notably, we proved that CDKL5 influences alternative splicing, at least as proved in heterologous minigene assays. In conclusion, we provide evidence that CDKL5 is involved indirectly in pre-mRNA processing, by controlling splicing factor dynamics. These findings identify a biological process whose disregulation might affect neuronal maturation and activity in *CDKL5*-related disorders.

INTRODUCTION

CDKL5 is an X-linked gene encoding a serine–threonine kinase. It belongs to the cyclin-dependent kinase-like (CDKL) family and shares partial homology with both MAP and cell cycle-dependent kinases (1,2). The gene was originally found disrupted in a balanced X-autosomal translocation in two unrelated female patients with a phenotype of severe infantile spasms syndrome X-linked (3). Subsequently, *CDKL5* mutations have been found in more than 50 patients exhibiting a large spectrum of neurological clinical manifestations including early neonatal encephalopathy, drug resistant infantile spasms, autism-like behaviour and severe mental retardation (4–10). Furthermore, *CDKL5* mutations are

*To whom correspondence should be addressed at: Stem Cells and Neurogenesis Unit, Division of Neuroscience, San Raffaele Scientific Institute, Via Olgettina 58, Milan 20132, Italy. Tel: +39 0226434616; Fax: +39 0226434621; Email: broccoli.vania@hsr.it

responsible for a specific form of Rett syndrome known as Hanefeld or early-onset seizure variant where mutations in *MeCP2* are only rarely identified. From a clinical point of view, the Hanefeld variant differs from the classic form of Rett syndrome in the absence of an apparent period of normal development while early-onset epileptic seizures are evident soon after birth. Patients also display some of the classical symptoms of Rett syndrome, such as loss of speech, stereotypic hand movements and microcephaly (11–14). Up to now, a number of *CDKL5* disease-causing mutations have been identified; however, a general genotype–phenotype correlation has not yet been established, leaving undetermined the genetic bases of this variability (8–10). Rare cases of boys with *CDKL5* mutations or genomic deletions encompassing the *CDKL5* gene have been described exhibiting a severe clinical phenotype with early-onset encephalopathy and intractable epilepsy (15,16). From these recent reports, it appears evident that *CDKL5* pathogenetic mutations are a significant cause in girls of severe early-onset neurodevelopmental disorders.

As mutations in *MECP2* and *CDKL5* are both associated with Rett syndrome, their involvement in a common pathway has been investigated. Interestingly, it has been shown that the two proteins are widely co-expressed in the brain and are similarly activated during neuronal maturation and synaptogenesis (12,17). At the molecular level, the two proteins interact together and CDKL5 mediates MeCP2 phosphorylation *in vitro* (12,18,19). However, it remains to be elucidated which residues are phosphorylated by CDKL5 and how MeCP2 activity is influenced by these modifications. Furthermore, a recent report has suggested a new link between CDKL5 and MeCP2. Both proteins have been shown, indeed, to bind to DNA methyltransferase 1 an enzyme that recognizes and methylates hemimethylated CpG dinucleotides after DNA replication to maintain a correct methylation pattern (19).

Despite this molecular correlation whose functional meaning remains to be ascertained, there are reasons to believe that CDKL5 also performs MeCP2-independent functions. As a matter of fact, *CDKL5* mutations are closely associated to some severe neurological symptoms, which are occasionally reported in typical MeCP2 diseases, such as infantile spasms, early-onset epilepsy and hypsarrhythmia. Furthermore, while MeCP2 is a nuclear protein, CDKL5 shuttles between the cytoplasm and nucleus through a CRM1-mediated nuclear export mechanism. Importantly, the relative concentration of CDKL5 in each cellular compartment varies in different brain areas and during development (17).

It has recently been demonstrated that a significant portion of the endogenous CDKL5 localizes in the nuclear compartment, where it displays a characteristic punctate staining. This has been shown for a number of cell lines and neural tissues (17,20). However, the exact identification of these nuclear sub-compartments and their functions in the nuclear processes has not yet been addressed.

Here, we report for the first time that CDKL5 localizes and is associated with a number of splicing factors that are clustered in structures called nuclear speckles. Moreover, CDKL5 nuclear distribution is not affected by inhibition of cellular transcription and is not mediated by the association with RNA. Regarding the physiological role of CDKL5 in nuclear speckles, we provide evidence that CDKL5, probably through its ability to regulate the nuclear trafficking of splicing factors, impairs the specificity of the splicing machinery. Our data, thus, demonstrate a new role of CDKL5 in nuclear organization and might provide novel important insights regarding the molecular mechanisms involved in Rett syndrome and related neurodevelopmental disorders.

RESULTS

The nuclear fraction of CDKL5 is highly enriched in the nuclear speckles

To investigate the subcellular localization of CDKL5, we performed indirect immunofluorescence with a polyclonal CDKL5 antibody. This has been previously prepared in our laboratory, and its specificity has been confirmed in various assays (17,20). In NIH3T3 cells as well as in HeLa cells, endogenous CDKL5 exhibited a diffuse nucleoplasmic pattern with an intense signal in organized granule-like sites (Fig. 1A and data not shown). No signal was observed with the pre-immune serum or when the incubation with the primary antibody was omitted. Moreover, a similar pattern of nuclear staining was also observed using an immunopurified serum. These findings indicate that the signal obtained in our experimental conditions was highly specific. The previously identified interaction between CDKL5 and MeCP2, suggested to us that the nuclear puncta of CDKL5 might correspond to MeCP2 positive heterochromatic foci. However, in Myc-MeCP2 transfected NIH3T3 cells, CDKL5 and MeCP2 did not co-localize, although rare double-positive puncta were occasionally observed (Fig. 1A–C, arrowheads). Accordingly, CDKL5-positive puncta did not localize with the intensively Hoechst stained pericentric foci, which distinguish methylated CpG-rich DNA (Fig. 1D and F, arrows). These results indicate that CDKL5 does not accumulate within the heterochromatin domains, as MeCP2 normally does. The staining pattern of CDKL5 was reminiscent of compartments enriched in RNA splicing and processing components referred to as nuclear speckles. These are discrete nuclear domains where pre-messenger RNA splicing factors, ribonucleoprotein particles (snRNPs), spliceosome subunits and non-snRNP protein splicing factors accumulate. Thus, it is well accepted that nuclear speckles act as storage compartments that can supply splicing factors to active transcription sites (21–23). To determine whether CDKL5 might colocalize with the nuclear speckles, we carried out immunofluorescence experiments with antibodies against CDKL5 and some splicing factors. SC35 is a non-snRNP splicing factor of the serine-rich (SR) family of proteins, while Sm (Smith antigen) associates with the snRNPs U1, U2, U4, U5 and U6 (21–23). Interestingly, the nuclear dots of CDKL5 were found to overlap with SC35 staining and a similar co-localization was obtained also with Sm (Fig. 1D–I). On the other hand, CDKL5 was detected either in the nucleolus, visualized by fibrillarin, staining or in the p80-coilin positive Cajal bodies (data not shown). Thus, CDKL5 accumulates in the splicing factor-rich nuclear speckles. The distribution of CDKL5 in the nucleus as well as the co-localization of CDKL5 with SC35 was also observed in 10 DIV primary

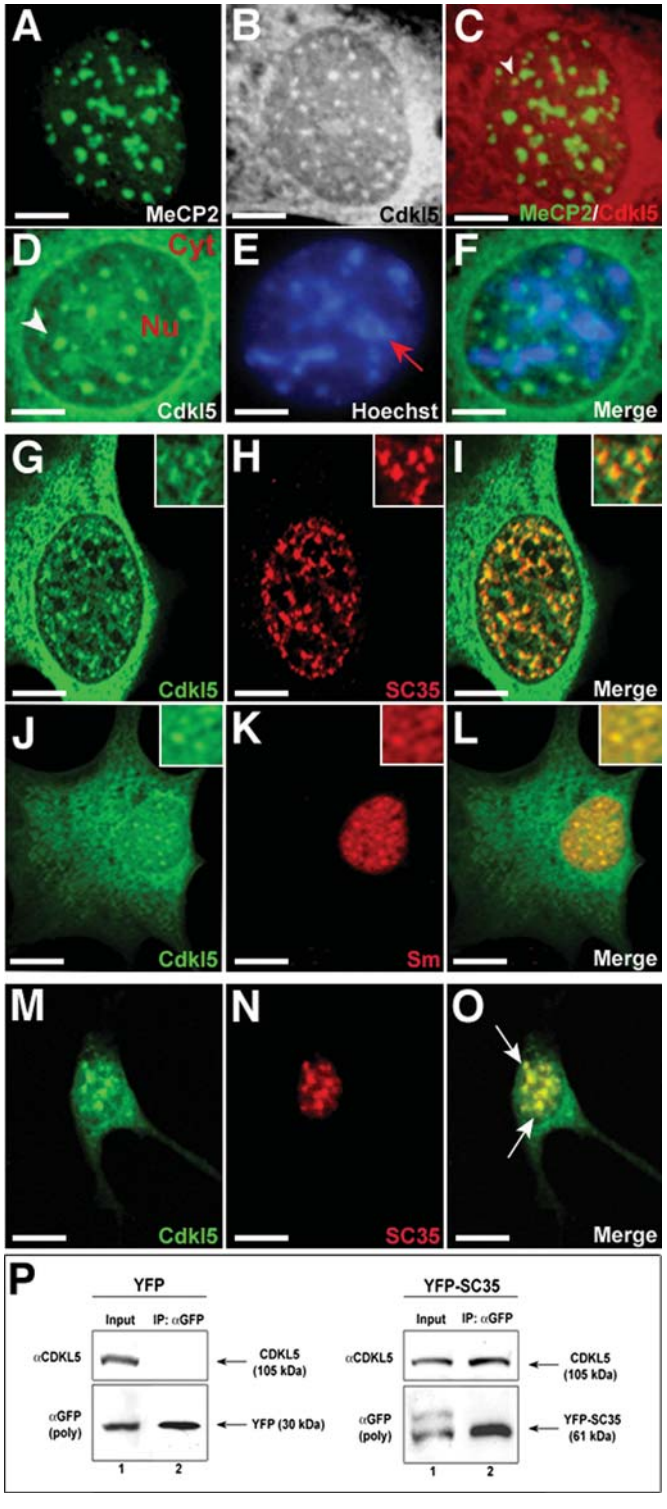

Figure 1. Nuclear CDKL5 accumulates into nuclear speckles. NIH3T3 cells were transiently transfected with Myc-MeCP2. 24 h post-transfection, cells were labelled for immunofluorescence with CDKL5 (**B**) and Myc antibodies (**A**) to detect endogenous CDKL5 and recombinant Myc-tagged protein. In (**C**), arrowhead point to a region of co-localization between CDKL5 and MeCP2. (**D** and **E**) Immunostaining of CDKL5 and Hoechst, respectively. (**F**) Merged image. In (D), arrowhead points to a CDKL5 nuclear foci. Arrow in (E) indicates heterochromatic foci. To show co-localization with speckle proteins, NIH3T3 cells and 10 DIV hippocampal neurons were stained with CDKL5 antibody (**G, J** and **M**), and either monoclonal SC35 (**H** and **N**) or Sm antibodies (**K**). (**I, L** and **O**) Merged images. In (O), arrows point the co-localization between CDKL5 and SC35 in hippocampal neurons. (**P**) CDKL5 and SC35 interact *in vitro*. Total cell lysates of NIH3T3 cells transfected with YFP (left panel) or YFP-SC35 (right panel) was subjected to immunoprecipitation (IP) with monoclonal anti-GFP antibody. Immunoprecipitated proteins as well 10% of the cell extracts were separated by electrophoresis and analyzed by immunoblotting using antibodies indicated on the left side of each panel. Scale bars: (A–I) 5 μm; (J–O) 10 μm.

mouse hippocampal neurons (Fig. 1J–L). To provide further evidence that CDKL5 associates with the nuclear speckles, we verified whether it could immunoprecipitate with the nuclear speckles component SC35. To this end, NIH3T3 cells were transiently transfected with both YFP (control) and YFP-SC35. The cells were recovered 16 h post-transfection, and total cell extracts were subjected to immunoprecipitation with a monoclonal anti-GFP antibody. Immunoprecipitated proteins were then separated by SDS–PAGE and visualized by immunoblotting with the polyclonal CDKL5 antibody. As shown in Figure 1M, the endogenous CDKL5 co-precipitated with YFP-SC35, but not with YFP.

Interestingly, CDKL5 exhibited a frank dot-like nuclear pattern at least in some tissues, as scored, for instance, in the principal CA1 neurons of the adult hippocampus (Supplementary Material, Fig. S1). This finding indicates that the spatial sub-nuclear compartmentalization of CDKL5 is also observable *in vivo*.

Altogether, these data indicate that in the nucleus CDKL5 localizes to nuclear speckles and is found in a complex with the SR protein SC35.

CDKL5 is an RNase-insensitive nuclear speckle component

Nuclear speckles are dynamic structures and act as storage/assembly/modification compartments that can supply splicing factors to active transcription sites. Their size, number and shape can change depending on the transcription levels in the cell and in response to environmental signals. The effects of RNA polymerase-II (Pol-II) inhibitors on the nuclear organization of splicing factors are well documented. For example, in cells treated with 5,6-dichloro-1-beta-D-ribobenzimidazole (DRB), which specifically inhibits Pol-II, nuclear speckles reduce in number, and concurrently enlarge dramatically and acquire a more rounded-like appearance (23). The same effects are seen with a-amanitin, another Pol-II inhibitor (23). To explore the possibility that also CDKL5-positive speckles might be modified by transcriptional inhibitors, NIH3T3 cells and primary hippocampal neurons were treated with DRB. Indeed, we observed a redistribution of CDKL5 speckles into enlarged foci upon DRB treatment, similar to that seen with SC35 or Sm (Fig. 2G–L; compare with untreated cells in Fig. 2A–F). DRB treatment of mouse primary hippocampal neurons produced a similar outcome with the accumulation of large CDKL5/SC35 double positive nuclear speckles (Fig. 2M–R). Similar results were obtained when transcription was halted using the Pol-II inhibitor a-amanitin (data not shown).

It is well established that the structural stability of nuclear speckles relies on two different types of protein interactions: one that is resistant to RNase treatment (e.g. SC35) and

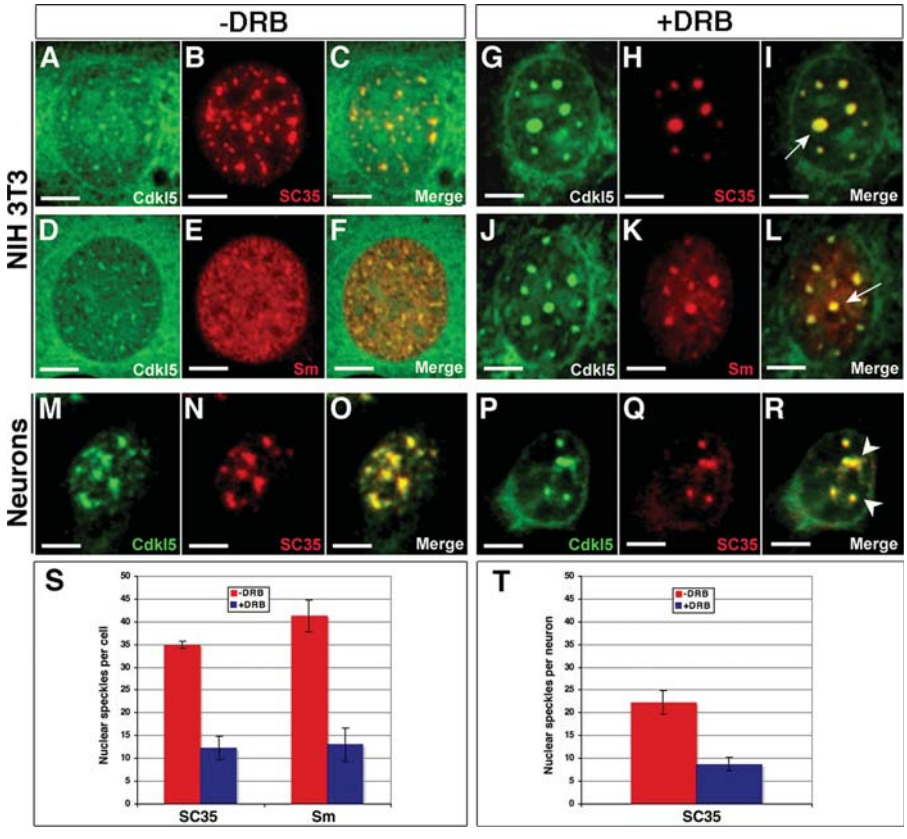

Figure 2. CDKL5 nuclear distribution is not affected by inhibition of cellular transcription. NIH3T3 cells and 10 DIV hippocampal neurons were either left untreated or treated with 100 μM 5,6-dicloro1-beta-D-ribobenzymidazole (DRB) in cell culture medium for 4 h at 37°C. Cells were then labelled for immunofluorescence with CDKL5 (**A, D, G, J, M** and **P**), SC35 (**B, H, N** and **Q**) and Sm (**E** and **K**) to detect endogenous proteins. (**C, F, O, I, L** and **R**) Merged images. In both cellular types, speckles labelled with SC35 and Sm antibodies became larger, rounded-up and overlapped with CDKL5. Arrows in (I, L) and arrowheads in (R) point to rounded-up nuclear speckles. (**S** and **T**) Quantification of the number of nuclear speckles for cells subjected to the indicated treatments. Quantification was performed visually by counting on the pictures the number of fluorescent foci in each cell. The values correspond to the means of three-independent experiments ($n = 40$ cells). Error bars represent standard deviations from the means. Scale bars: 5 μm.

another that is RNase sensitive (e.g. snRNPs identified with the Smith antigen-recognizing antibody Y12). To evaluate the nature of the association of CDKL5 with the nuclear speckles, NIH3T3 cells were permeabilized, fixed and then treated with RNase (100 μg/ml, 2 h). The staining pattern of CDKL5 resulted unaffected after RNA degradation, as scored for SC35 immunoreactivity (compare Supplementary Material, Fig. S2A, B with S2E, G). On the contrary, Sm staining became completely diffuse after RNase treatment (compare Supplementary Material, Fig. S2D with S2H). These results demonstrate that CDKL5 association to nuclear speckles is not mediated through binding to RNA, but depends on protein–protein interactions.

Overexpression of CDKL5 causes redistribution of nuclear speckle components

It is well established that the dynamic association of SR proteins to nuclear speckles is strictly dependent on their phosphorylation state. Indeed, it has been shown that phosphorylation of the RS domain of SR splicing factors is necessary for their release from speckles to sites where pre-mRNA splicing processing takes place. Several protein kinases have been described that can phosphorylate the RS domain of SR proteins and the two most extensively studied are SRPK1 and Clk/STY (24,25). Transfection assays provide evidence that both kinases, SRPK1 and Clk/STY, with the dual specificity to phosphorylate both Ser/Thr and Tyr residues, can target different components of the nuclear speckles resulting in the complete redistribution of splicing factors from speckles to a diffuse nuclear pool (26–28). The above observations leave open the possibility that also CDKL5, as a Ser/Thr protein kinase, could have a role in nuclear speckle maintenance. To address this question, NIH3T3 cells were transfected with a CDKL5 cDNA fused to GFP and 16 h post-transfection the nuclear speckles morphology was analyzed by indirect immunofluorescence. Interestingly, in cells expressing GFP-CDKL5, we observed a dramatic reduction of SC35 staining, which remained confined to only small and fading foci (Fig. 3B and D, arrowhead in B), whereas in neighbouring non-transfected cells SC35 maintained its normal localization in the nuclear speckles (Fig. 3B and C, arrow in C). To test whether this effect of CDKL5 overexpression on speckles was general or specific for SC35, we investigated the response of proteins that localize to nuclear speckles but are not members of the SR protein family. To this end, we stained cells for Sm, which recognizes components of the snRNPs. Similar to that we observed for SC35, in CDKL5 overexpressing cells, Sm posi-

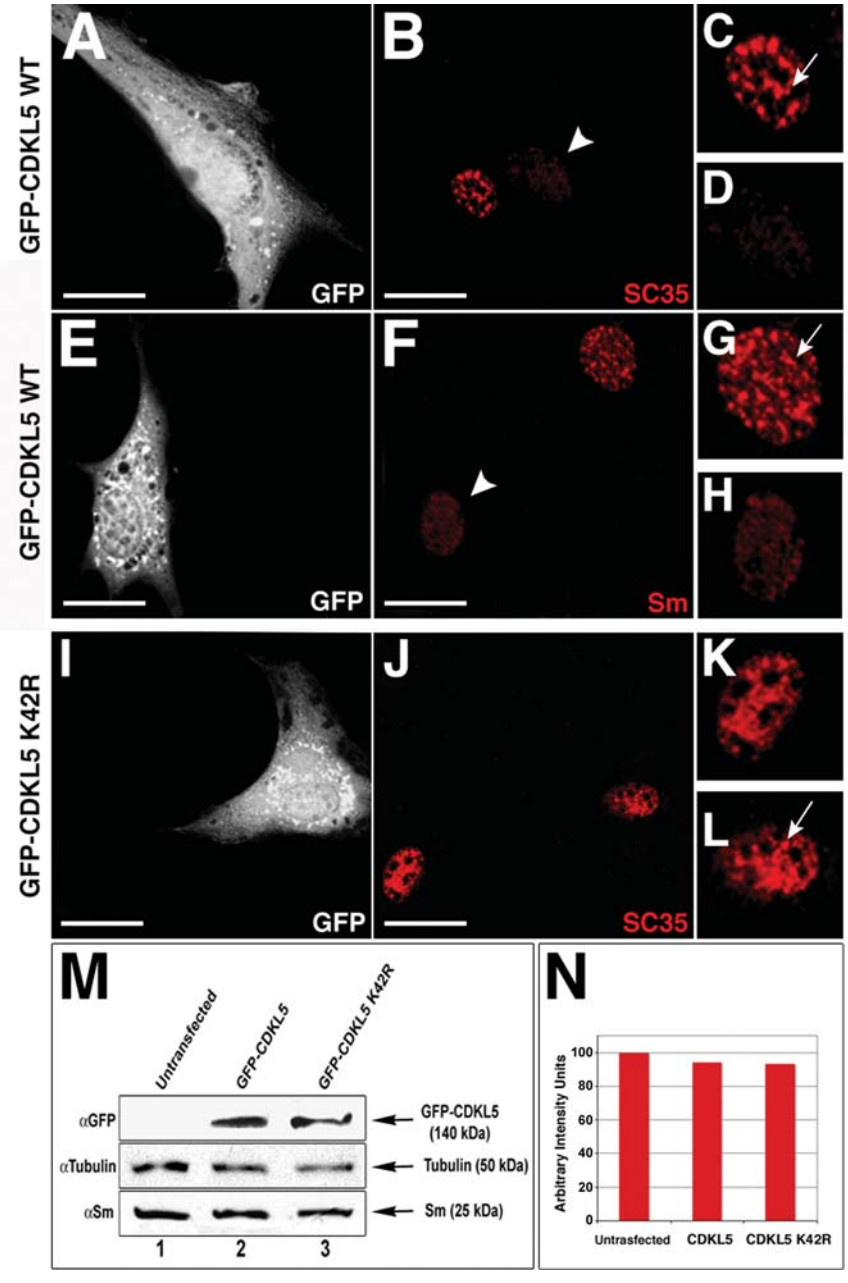

Figure 3. CDKL5 overexpression induces nuclear speckle components redistribution. NIH3T3 cells were transfected with either GFP-CDKL5 WT (**A** and **E**) or GFP-CDKL5 K42R (**I**). Staining for GFP (A, E, I), SC35 (**B, J**), and Sm (**F**) was performed 16 h after cell transfections. NIH3T3 cells transfected with GFP-CDKL5 WT show redistribution of both SC35 (B) and Sm (F) to a diffuse nuclear localization (arrowheads), in contrast to untransfected cells or cells transfected with GFP-CDKL5 K42R in which SC35 is clearly localized in nuclear foci (**C, G, K, L,** arrows). (C, **D,** G, **H,** K and L) Enlargements of the regions pointed by arrowheads. In (C, G and L), arrows point to a nuclear speckle. (**M**) NIH3T3 cells were left untransfected (lane 1) or were transfected with GFP-CDKL5 WT (lane 2) or GFP-CDKL5 K42R (lane 3) and extracts analyzed by immunostainngs for GFP, Tubulin and Sm antibodies, showing no differences in the levels of Sm. (**N**) Densitometric scanning quantification of the relative abundance of Sm in each fraction is presented in a bar graph. Scale bars: 5 μm.

tive dots became dimmer and less distinct throughout the nucleus (Fig. 3F–H, arrowhead in F). It is worthwhile to note that the nuclear fraction of over-expressed CDKL5 was not completely confined in dots but also distributed uniformly in the nucleoplasm, as judged by the diffuse GFP signal, supporting the nuclear speckles disassembly hypothesis (Fig. 3A). At this point, we asked whether the catalytic activity of CDKL5 was required for the effect of the kinase on nuclear speckle stability. Therefore, the kinase-dead mutant of CDKL5 (p.K42R), which has previously been shown to be completely devoid of phosphorylation activity, was overexpressed in NIH3T3 (20). In contrast to the wild-type (WT) CDKL5, the catalytically inactive mutant of CDKL5 was still noted in nuclear speckles and failed to trigger any evident alteration in the SC35 staining (Fig. 3I–L, arrow in L). These results suggest that CDKL5 does indeed cause disassembly of nuclear speckles in a kinase-

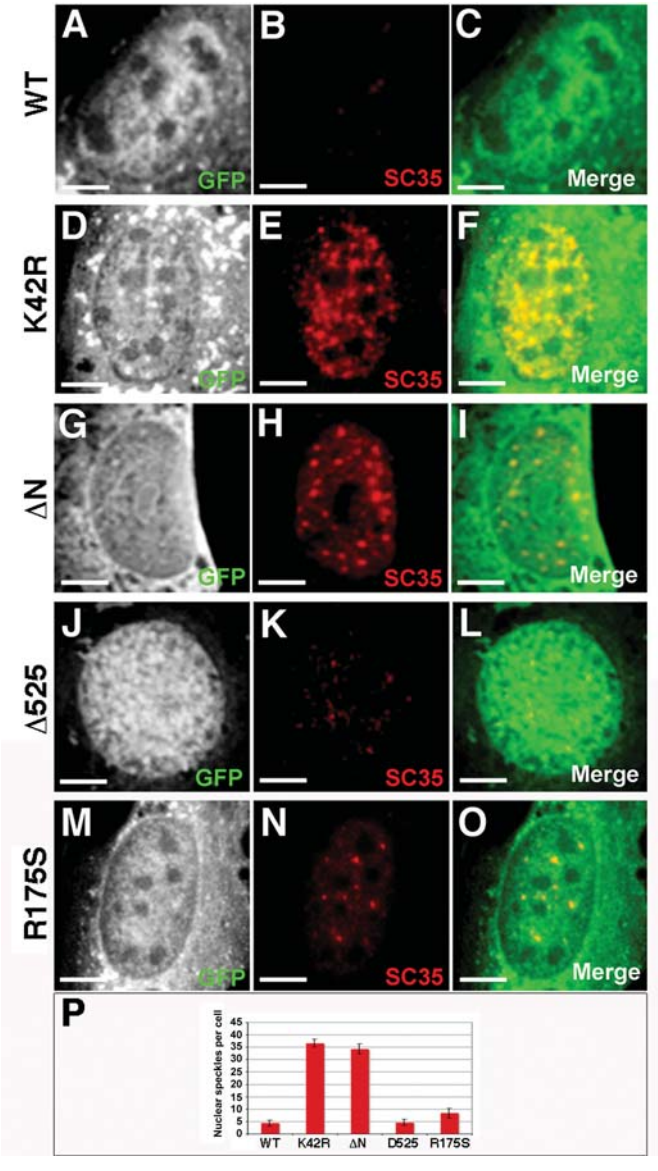

Figure 4. The catalytic domain of CDKL5 is required and sufficient for nuclear speckles redistribution. NIH3T3 cells were transiently transfected with each deletion mutants fused to GFP and then labelled for immunofluorescence with GFP (**A, D, G, J** and **M**) and SC35 (**B, E, H, K** and **N**) antibodies. (**C, F, I, L** and **O**) Merged images. (A–C) Overexpression of the CDKL5 wild-type (WT) form exerts a profound disassembly of the SC35-positive nuclear speckles. (D–I) CDKL5 mutants K42R (D–F) and DN (Δ1-297aa) (G–I) lacking the kinase activity do not exert any evident changes in nuclear speckle distribution after exogenous expression. (J–L) NIH3T3 cells overexpressing the D525 CDKL5 mutant form, which lack all the C-terminal domain of the protein, exhibit a strong loss of SC35 immunoreactivity. (M–O) Forced expression of the pathogenic CDKL5 allele with a missense mutation in the catalytic domain (R175S) is able to notably reduce the number of SC35-positive nuclear puncta. The number of nuclear speckles in transfected cells is represented in the chart (**P**). The values correspond to the means of four-independent experiments ($n = 50$ cells). Error bars represent standard deviations from the means. Size bars: 5 μm.

dependent manner, resulting in a redistribution of at least some speckle proteins. We reasoned that the reduction of SC35 and Sm positive puncta might be the result of degradation of these proteins or their redistribution throughout the nucleoplasm. To address this issue, immunoblotting with Sm antibody was performed on extracts of cells transfected with either GFP-CDKL5 or GFP-CDKL5-K42R. In all three conditions, the total amount of Sm protein was found not evidently changed, suggesting that the loss of Sm positive puncta is caused by a redistribution of the protein throughout the nucleoplasm. Together, these findings establish a role of CDKL5 in regulating the dynamic behaviour of nuclear speckles.

CDKL5 disease-causing mutations affect nuclear speckle structures

To further understand how CDKL5 exerts its function, we wished to examine the effects on nuclear speckle organization of different CDKL5 synthetic or disease-causing mutants. Interestingly, the ΔN-CDKL5 mutant (p.M1_F297del), lacking the entire kinase domain, did not affect nuclear speckle disassembly similar to what was observed with the K42R kinase-dead mutant (Fig. 4A–I). On the contrary, a CDKL5 mutant lacking most of the C-terminal region (Δ525), but preserving catalytic activity did induce the redistribution of both SC35 and Sm, at a similar level to WT CDKL5 (Fig. 4J–L and data not shown). These findings indicate that CDKL5 kinase activity is necessary and sufficient for regulating nuclear speckle homeostasis. Subsequently, we analyzed the effect on nuclear speckle disassembly, of a CDKL5 disease-causing missense mutations, p.R175S (c.525A>T), that has been previously associated with encephalopathy and early-onset variant of Rett syndrome (4). This mutation is particularly interesting since it has been previously described to retain part of its autocatalytic activity and, therefore, to function as a hypomorphic mutant (17,18). Interestingly, overexpression in NIH3T3 cells of the p.R175S mutant induced a loss of SC35 puncta, although the reduction was less dramatic compared with CDKL5 WT (Fig. 4M–O). This indicates that the p.R175S mutant, although exhibiting a reduced kinase activity, is still able to notably affect nuclear speckle organization when overexpressed. On the basis of the results obtained for the kinase-defective mutants, it seems that the effect on splicing factor redistribution is strictly dependent on CDKL5 kinase activity.

CDKL5 is necessary for proper coalescence of nuclear speckle components

The results described above demonstrate for the first time that CDKL5 is present in nuclear speckles and suggest a specific function of the kinase in this sub-nuclear domain. Therefore, to gain insights into this role, we analyzed the effect of the absence of CDKL5 on nuclear speckle morphology, by means of short-hairpin RNA (shRNA) mediated silencing technology. To validate the CDKL5 shRNA, NIH3T3 cells and hippocampal neurons were transfected with either CDKL5 shRNA or, as control, a scrambled shRNA. The cells were recovered 48 h post-transfection and the levels of CDKL5 analyzed both by indirect immunofluorescence and by immunoblotting (Supplementary Material, Fig. S3G). The immunofluorescence experiments clearly showed that even if CDKL5 was not completely depleted, its levels were significantly reduced in CDKL5 shRNA treated cells compared

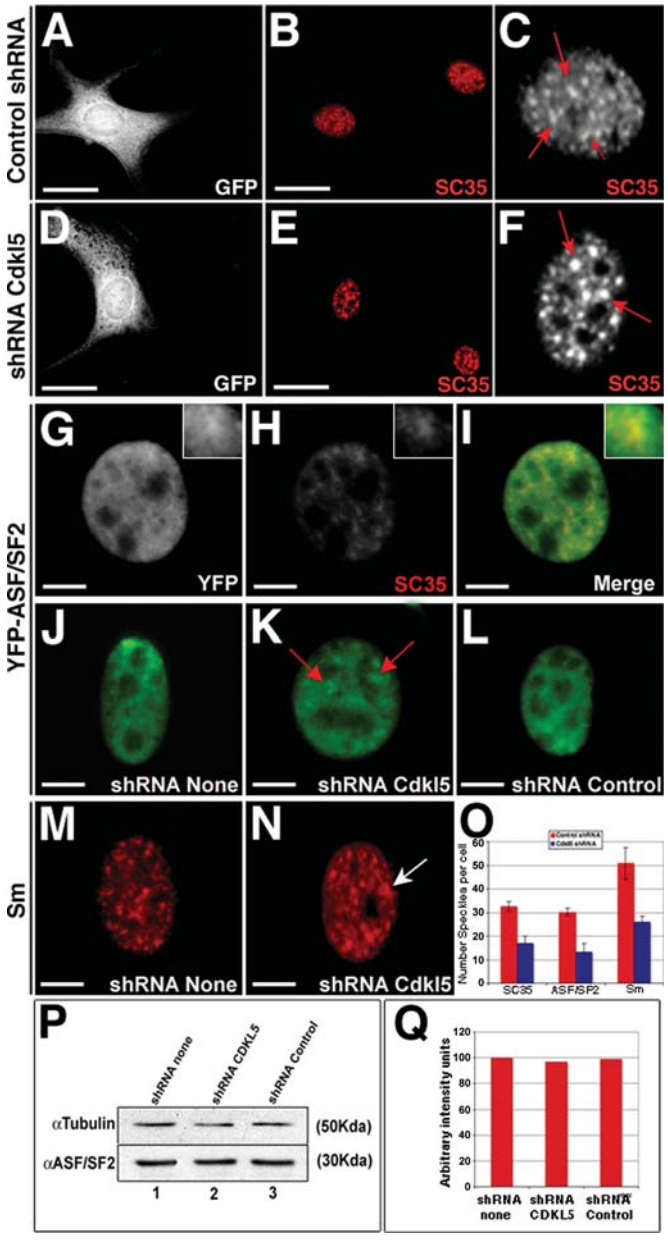

Figure 5. CDKL5 knockdown results in larger nuclear speckles. NIH3T3 cells were transfected with control shRNA or CDKL5 shRNA. Cells were recovered 48 h post-transfection and labelled for immunofluorescence with GFP (**A** and **D**) and SC35 antibodies (**B** and **E**). (**C** and **F**) Higher magnification of the transfected cell nuclei. Arrows in (C) point to nuclear speckles. Arrows in (F) point to rounded-up speckles. To show co-localization between ASF/SF2 and SC35, NIH3T3 cells were transfected with YFP-ASF/SF2 and stained with GFP (**G**) and SC35 (**H**) antibodies. (**I**) Merged image. NIH3T3 cells were transfected with YFP-ASF/SF2 alone (**J**) or in combination with CDKL5 shRNA (**K**) or control shRNA (**L**), followed by immunostaining with GFP antibody. Arrows in (K) point to rounded-up nuclear speckles. Nuclear speckles were visualized by indirect immunofluorescence with Sm antibody in NIH3T3 cells left untransfected (**M**) or transfected with CDKL5 shRNA (**N**). In (N), arrow indicates a rounded-up nuclear speckle. (**O**) Quantification of the number of nuclear speckles of cells treated with either shRNA control or CDKL5 shRNA. Quantification was performed visually by counting on the pictures the number of fluorescent foci in each cell. The values correspond to the means of three-independent experiments ($n = 100$ cells). Error bars represent standard deviations from the means. (**P**) NIH3T3 cells were left untransfected (lane 1) or were transfected with control shRNA (lane 2) or CDKL5 shRNA (lane 3). Cells were recovered 48 h post-transfection and the expression levels of endogenous ASF/SF2 were analyzed by immunoblotting with ASF/SF2 antibody. (**Q**) Densitometric scanning quantification of the relative abundance of ASF/SF2 in each fraction is presented in a bar graph. Scale bars: (A, B, D, E) 10 μm; (G–N) 5 μm.

with control cells (Supplementary Material, Fig. S3C–F and data not shown). A densitometric analysis of the immunoblotting signals estimated that the levels of endogenous CDKL5 were reduced by ∼60% in CDKL5 shRNA treated cells with respect to control cells (Supplementary Material, Fig. S3H). Subsequently, we assessed whether CDKL5 knockdown could trigger any alteration in nuclear speckle morphology. Notably, the majority of CDKL5 silenced NIH3T3 cells presented larger and brighter nuclear speckles as highlighted by SC35 staining (Fig. 5D–F). Conversely, in cells transfected with the scrambled shRNA (control shRNA), SC35-positive nuclear speckles were not apparently affected in their size (Fig. 5A–C). To investigate whether other components of nuclear speckles were affected by interfering with CDKL5, the localization of ASF/SF2 and Sm were investigated. Overexpression of the SR family member ASF/SF2 fused to YFP permits to visualize nuclear speckles, where it accumulates without affecting their activity (Fig. 5G) (23). In contrast to untransfected cells or cells transfected with scrambled shRNA (Fig. 5G–L, arrows in K), ASF/SF2-YFP staining was detected in larger domains in cells interfered for CDKL5 cells (Fig. 5G–L, arrows in K). Likewise, Sm staining coalesced into larger nuclear domains in CDKL5 silenced, but not in control cells (Fig. 5M and N). The above results clearly indicate that CDKL5 knockdown induces an alteration of nuclear speckles morphology, suggesting that endogenous CDKL5 is necessary for nuclear speckle organization. To test whether the effect of CDKL5 knockdown was caused by a general gain in protein synthesis or protein re-localization, we analyzed by immunoblotting the expression levels of the endogenous ASF/SF2 protein. As in the case of CDKL5 overexpression, the down-regulation of the kinase did not lead to appreciable changes in the ASF/SF2 protein levels. Indeed, in both CDKL5 silenced and control cells ASF/SF2 protein levels were found unchanged (Fig. 5O). Altogether, our results indicate that CDKL5 down-regulation impacts nuclear speckle integrity.

CDKL5 mutant human primary skin fibroblasts show abnormal morphology of nuclear speckles

Thus far, the presented results revealed an unsuspected role of CDKL5 in the homeostasis of nuclear speckles. To analyze whether pathogenic Rett (RTT)-causing mutations in *CDKL5* influence this aspect, the above described experiments were also conducted on primary cells of *CDKL5*-mutated patients. The distribution of both the endogenous CDKL5 and SC35 was analyzed by indirect immunofluorescence in fibroblasts of a girl carrying a premature stop codon (p.R59X) in the *CDKL5*-coding region. This patient developed hypotonia and pharmacological resistant myoclonic seizures within the first year of life, followed by stereotypic hand movements without noting regression (see Materials and Methods).

Control fibroblasts were obtained from two girls of 6 and 10 years old with a suspected myopathy, who resulted healthy

after skin biopsy diagnostic examination. Interestingly, in control human fibroblasts CDKL5 staining showed the same features as observed both in NIH3T3 cells and in hippocampal neurons. As inferred from Figure 6A–C, CDKL5-positive nuclear foci resulted virtually coincident with the SC35-positive nuclear domains. These data indicate that the localization of CDKL5 in nuclear speckles is a conserved feature of the protein in both mouse and human cells. Subsequently, we analyzed nuclear speckle morphology in CDKL5 mutant fibroblasts (p.R59X). These mutant fibroblasts did not show any specific staining for CDKL5, indicating a complete loss of functional protein. Simultaneously, *CDKL5* mutant fibroblasts exhibited extremely large SC35-positive nuclear domains. In particular, SC35 nuclear foci appeared fewer, larger and less dot-like (Fig. 6D). Similar nuclear speckle altered morphology was observed in fibroblasts isolated from a second patient carrying a pathogenetic L220P CDKL5 mutation (p.L220P) (Fig. 6E). Since CDKL5 mutation is heterozygous, we scored both positive and negative CDKL5 cells within the same patient specific fibroblast cell population. Interestingly, CDKL5-positive cells displayed a normal content of SC35-positive nuclear speckles with a morphology resembling that described in control fibroblasts (Fig. 6F).

Results obtained with NIH3T3 cells together with results reported above consistently point to a key role of CDKL5 in regulating nuclear speckle homeostasis. The finding that CDKL5 down-regulation results in more round-up nuclear speckles suggests that reduced phosphorylation of yet unknown targets is most likely at the origin of this effect. Specifically, we interpret these nuclear foci as nuclear speckles where splicing factors accumulate to a great extent leading to a drastic increase of the speckle size.

To verify the effects of CDKL5 overexpression in patient cells, we transfected CDKL5 human fibroblasts (p.R59X) with GFP-CDKL5 and analyzed nuclear speckles morphology as previous by visualizing SC35. Interestingly, mutant fibroblasts overexpressing GFP-CDKL5 showed a drastic loss of SC35 staining, when compared with the non-transfected cells (Fig. 6H–K). The ability of exogenous GFP-CDKL5 to induce disassembly of nuclear speckles in fibroblasts devoid of the kinase, confirms a crucial role of CDKL5 to regulate the stability of these structures.

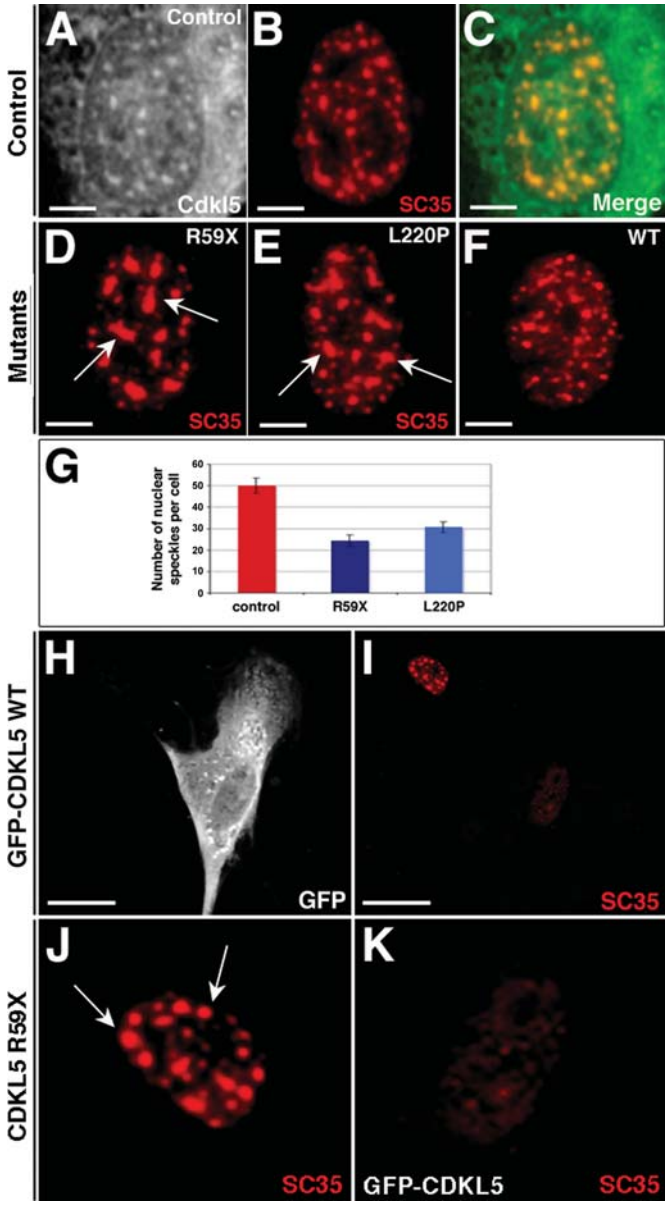

Figure 6. Nuclear speckles morphology in patient-specific primary fibroblasts. Human fibroblasts, CDKL5 R59X and CDKL5 L220P fibroblasts were immunostained with CDKL5 (**A**) and SC35 (**B, D, E** and **F**) antibodies. (**C**) Merged image. (**G**) Quantification of the number of nuclear speckles per cell. Quantification was performed visually by counting on the pictures the number of fluorescent foci in each cell. The values correspond to the means of three-independent experiments ($n = 50$ cells). Error bars represent standard deviations from the means. CDKL5 R59X fibroblasts were transfected with GFP-CDKL5 WT and then stained with GFP (**H**) and SC35 (**I**) antibodies. Higher magnification of untransfected (**J**) and transfected cell nuclei (**K**) is shown. Arrows in (J) show rounded-up nuclear speckles. Scale bars: (A–F) 5 μm; (H, I) 10 μm.

CDKL5 overexpression affects splicing of a reporter minigene

Splice site selection and pre-mRNA splicing are dynamic processes that involve constant remodelling of splicing factors, such as SR proteins, on the pre-mRNA being processed. In particular, alterations in the concentration of SR proteins in areas where splicing occurs are thought to be critical for the control of pre-mRNA splicing (29–31). It is by now well established that phosphorylation events can modify the subcellular localization of these regulatory proteins. This alters their relative concentration at transcription sites, resulting in a change in splice site selection. There are several pieces of evidence that a number of kinases are able to phosphorylate SR proteins (23,30). Furthermore, at least one of these, Clk/STY, can modulate splicing *in vitro* (23). Therefore, it would be conceivable that also CDKL5 might be involved in pre-mRNA splicing. To address this question, we performed an *in vivo* splicing assay using the Adenovirus E1A minigene. In general, transfection of the adenovirus E1A construct into cultured cells generates multiple RNA isoforms (9S, 12S and 13S) due to the utilization of alternative 5′ splice sites, rendering it frequently employed as a reporter for alternative

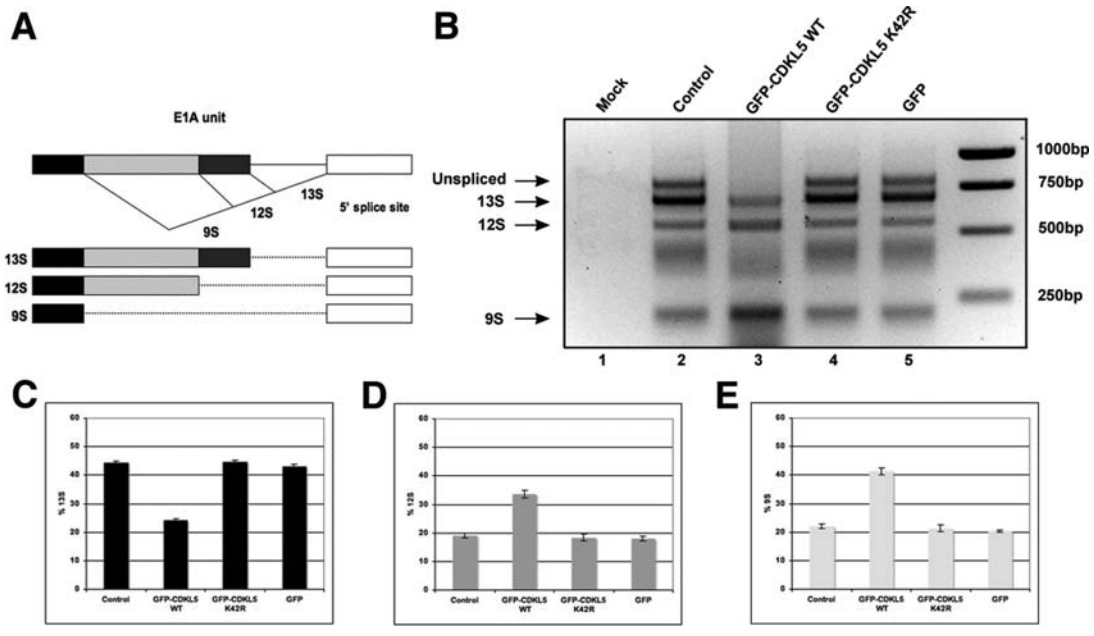

Figure 7. CDKL5 affects E1A minigene splicing *in vivo*. (**A**) Schematic representation of the Adenovirus E1A minigene splicing pattern. Three splice isoforms (13S, 12S and 9S) are produced by different 5′ splice site selection. (**B**) NIH3T3 cells were left untransfected (lane 1) or were transfected with the E1A reporter (lane 2) alone or in combination with GFP-CDKL5 WT (lane 3), GFP-CDKL5 K42R (lane 4) or GFP (lane 5). Total RNA was extracted and analyzed by RT–PCR and 1.5% agarose gel electrophoresis. The positions of size standards are indicated on the right. (**C**–**E**) Quantitative analysis. The relative amounts of the splice products (13S, 12S and 9S) were measured by densitometric scanning and the percentage of each isoform is expressed as the average with SEM ($n = 3$).

splicing (Fig. 7A) (32–34). The E1A minigene was transfected into NIH3T3 cells in combination with vectors expressing GFP-CDKL5, GFP-CDKL5-K42R or GFP alone. The presence of different splicing products was examined by semi-quantitative RT–PCR. As shown in Figure 7B, CDKL5 overexpression caused an increase of 9S and 12S isoforms and a concomitant decrease of the 13S isoform together with the unspliced pre-mRNA. Furthermore, we found that the selection of the 9S 5′ splice site selection is stimulated by the catalytic activity of CDKL5 since the overexpression of the kinase dead mutant (K42R) had no effect on the splice site selection (Fig. 7B–E). These findings illustrate the involvement of CDKL5 in the complex machinery regulating pre-mRNA spliceosome activity and alternative splicing.

DISCUSSION

The involvement of CDKL5 in the aetiology of several neurodevelopmental disorders, including early-onset encephalopathy, infantile-spasms and atypical RTT, underscores the importance of this protein in neuronal function. However, its function is far from being entirely understood, precluding an understanding of its role in the pathogenetic processes. Herein, we describe a novel and unexpected role of CDKL5 in the structural organization of nuclear speckles and the dynamics of their components. Surprisingly, CDKL5 ectopic expression is sufficient to induce disassembly of the speckles in both, cell lines and primary human fibroblasts. Conversely, its down-regulation obtained by means of shRNA-mediated silencing technology leads to consistent larger speckles. Accordingly, *CDKL5*-mutated human primary fibroblasts display abnormally large and uneven speckles. Together, these results indicate that CDKL5 plays an important role in the correct maintenance of speckle structures.

It is by now well known that a number of kinases act on nuclear speckles morphology in a similar way as described here for CDKL5. In fact, misexpression of different members of the Clk/STY and SRPK kinase families lead to a severe disassembly of nuclear speckles (24,25,27). Speckles are thought to be the result of the aggregation of pre-mRNA splicing factors, including ribonucleoprotein particles (snRNPs) and arginine–serine-rich splicing factors. SR proteins constitute a large family of highly evolutionary conserved factors. These factors present a similar structure with an N-terminal RNP type RNA binding domain and a C-terminal region enriched in repeated arginine–serine dipeptides (RS domains) (26,27). Phosphorylation of serines within the RS domains control their sub-nuclear localization and binding to RNA. In fact, overexpression of SR-specific Clk/STY and SRPK kinases elicit SR proteins to be released from nuclear speckles and reach the active site of transcription where they are assembled into the spliceosome (24,25,27). Therefore, nuclear speckles should be considered highly dynamic structures existing in equilibrium between continuing assembly and disassembly of their protein components (21–23).

Interestingly, the alterations of nuclear speckles caused by CDKL5 misexpression appear mostly dependent by its kinase activity as inferred from the results obtained upon misexpression of different mutant derivatives. These results

suggest that CDKL5 might exert a control on these subnuclear structures by influencing the cycle of phosphorylation and dephosphorylation of their associated SR proteins. Future studies will be aimed to identify which of the numerous SR proteins or, perhaps, other related nuclear speckle factors, function as direct targets of CDKL5 mediating its effect on speckles morphology.

We reported that CDKL5 misexpression influences alternative splicing of the Adenovirus E1A minigene, which in general produces three major splice isoforms, depending on different 5′ splice sites (Fig. 7). It is well established that alternative splicing is controlled by the type and amount of SR proteins readily available at the sites of mRNA processing. Indeed, the relative abundance of each single specific SR protein and the molar ratio of each SR protein with respect to their specific antagonists (e.g. hnRNP A/B family members) determine the patterns of alternative splicing (28,35–37). For example, increasing the concentration of ASF/SF2 favours usage of the most downstream 5′ splice site in mRNAs containing alternative 5′ splice sites (38). It is, therefore, plausible, that the control of alternative splicing mediated by CDKL5 is reached by influencing the delicate equilibrium between the two pools of pre-mRNA splicing factors associated to nuclear speckles or to the spliceosome. Supporting this hypothesis, overexpression of the kinase-dead CDKL5 mutant (K42R) was unable to elicit any alteration in the splicing pattern of the E1A minigene, indicating that downstream events of protein phosphorylation are necessary for CDKL5 to regulate splicing activity.

Despite the fact that CDKL5 has been shown to work in a pathway common with that of MeCP2 (12), there are reasons to believe that CDKL5 also performs MeCP2-independent functions. In this work, we describe a specific function played by CDKL5 in regulating nuclear speckle homeostasis, which has never been associated with MeCP2. Indeed, unlike MeCP2, CDKL5 is closely associated with and can alter the morphology of these nuclear structures. Thus, herein, we described the first MeCP2-independent CDKL5 function in this specific biological complex. We hypothesize that any CDKL5 dysfunction in this process results in an imbalance of the various components of the spliceosome machinery, which ultimately leads to alterations of the splicing pattern of a number of undefined RNA transcripts.

Therefore, CDKL5 dysfunction might cause a general alteration in RNA processing and splicing regulation, which could be particularly deleterious for the maturation, function or survival of brain neurons. To our knowledge, CDKL5 is the first non-snRNP associated nuclear speckle protein mutations in which are responsible for neurological disorders. In fact, whereas mutations causing retinal degeneration have been described in the genes PRPF31, PRPF8 and PRPF3 coding for proteins of the snRNPs complexes (39), no mutations in other components of the nuclear speckle structures have yet been found responsible for other human genetic disorders. Aberrant RNA processing associated with both neuronal cell death and neurological symptoms have been described in individuals with mutations in the *SMN1* or *TARDBP* (*TDP43*, *ALS10*) genes, causing spinal muscular atrophy and amyothrophic lateral sclerosis, respectively (40). Both *SMN1* and *TARDBP* encode hnRNP-associated proteins with a presumptive role in controlling splicing pattern activity (41,42). Interestingly, in SMN1-deficient mice, aberrant alternative splicing was observed in various tissues and for numerous genes, even though this global alteration is coupled with the only specific degeneration of motor spinal neurons (43). However, RTT is distinct with respect to these pathologies, since it has been reported to lack a clear association with its pathological course and any notable neuronal cell death process (44).

Intriguingly, MeCP2 itself has been also involved in regulating alternative splicing. Indeed, MeCP2 is able to regulate splicing of reporter minigenes, probably trough its direct interaction with the RNA-associated protein YB1 (45). Most importantly, MeCP2 mutant animals displayed aberrant splicing for a number of target genes expressed predominantly in the brain (45). Thus, both CDKL5 and MeCP2 have roles in RNA processing regulation although with apparently different molecular mechanisms. However, it might be possible that direct links exist between CDKL5 and MeCP2 dependent regulation of RNA processing. Considering these result, it might be proposed that classical, early-onset RTT and similar CDKL5-dependent neurodevelopmental disorders might be the results of an aberrant RNA metabolism particularly deleterious for neuronal function.

Future experiments, including development of *in vivo* model systems, will be essential in sorting out the impact of the CDKL5-regulated mechanisms impinging on RNA processing during neuronal maturation and activity.

MATERIAL AND METHODS

Patient ascertainment

Patient with the R59X-mutated CDKL5 was the third child of healthy, unrelated parents. The first children were normal. She was born at term after an uneventful pregnancy. Her birth weight was 2720 g, height 46 cm and head circumference 32 cm. During the first weeks of life, the mother noted poor visual contact. When she was 2 months old, she was referred to a paediatric hospital for an acute gastroenteritis. At that time, hypotonia and seizures were noted. She had head control at 9 months, sat at 3 years but did not achieve independent walking. Hand use was limited to gross manipulation and she was unable to transfer objects from one hand to the other. She had no speech. She developed generalized tonic–clonic and myoclonic epilepsia. Seizures were brief, lasting <1 min but frequent (2 or 3 per day) and refractory to medication. EEG showed paroxysmal activity with generalized spikes on a low background rhythm. She had midline stereotypic hand movements and auto aggressive behaviour (biting) but no regression. She had an early and severe gastro oesophageal reflux and was predominantly fed by a gastrostomy tube. A severe scoliosis was treated surgically at the age of 14 years. Physical examination at the age of 17 years showed poor eye contact and poor eye fixation, strabismus, nystagmus and spastic paraparesis. The height and head circumference were on 2.5 SD, the weight on 4 SD. Additional features included very small feet and hands and some dysmorphic features:

wide nasal bridge, broad nasal tip, down slanting palpebral fissures and malar hypoplasia.

Cell culture and transfection

NIH3T3 cells, HeLa cells, human fibroblasts were maintained in Dulbecco's modified Eagle's medium (Invitrogen, Eugene, OR, USA) supplemented with 1% penicillin–streptomycin (Sigma-Aldrich, St Louis, MO, USA), 2 mM glutamine (Sigma-Aldrich) and 10% fetal bovine serum (Invitrogen) at 37°C with 5% CO_2. Transient DNA transfections were carried out using calcium phosphate precipitation method or Lipofectamine Plus Reagent (Invitrogen), according to manufacturer's instructions and cells harvested 16–48 h post-transfection. Cells were treated with DRB at 100 μM for 4 h and with a-amanitin at 50 μg/ml for 5 h.

Primary hippocampal cultures

Primary neuronal cultures were prepared from the hippocampus of day 17.5 mouse embryos (E17.5). Briefly, hippocampi were dissected from mouse brains under a dissection microscope and treated with trypsin (Invitrogen) for 15 min at 37°C before triturating mechanically with fire-polished glass pipette to obtain a single-cell suspension. Approximately 7×10^4 cells were plated on coverslips coated with poly-L-lysine in 12-well plates and cultured in Neurobasal medium (Invitrogen) supplemented with B27 (Invitrogen) and glutamine (Sigma-Aldrich). Neurons were fixed for immunostaining at 10 days after plating.

Plasmids and RNAi

pGFP-hCDKL5, pGFP-K42R, pGFP-ΔN, pGFP-Δ525, pGFP-C152F and pGFP-R175S were described previously (20). pE1A was a kind gift of D. Gabellini, pYFP-SC35 and pYFP-ASF/SF2 was kindly provided by D. Spector.

RNAi was performed using shRNAs expressed by pU6-mir30 vector. To generate shRNA-expressing plasmids, we have designed three different target sequences for the target CDKL5 gene and a mismatch sequence, which have subsequently been inserted into pU6-mir30 vector at *Eco*RI and *Xho*I restriction sites. The so prepared constructs were verified by DNA sequencing. The following targeted sequences were designed: CDKL5 shRNA no. 1 (CATTGG TAATGTGATGAATAAA), CDKL5 shRNA no. 2 (GGG ACATTATTTCCCTGCTTAC), CDKL5 shRNA no. 3 (AACACTGACGGTCCTGATCTAT). For CDKL5 shRNA validation, NIH3T3 cells were plated in six-well plates and transfected with 3 μg of shRNA plasmid and 1 μg of an appropriate reporter gene, using Lipofectamine Plus Reagent (Invitrogen), according to manufacturer's instructions. The reporter used was: pCAGGS-GFP. Cells were monitored for 48 h following transfection and the expression levels of endogenous CDKL5 analyzed by immunofluorescence and immunoblotting. Among the three shRNA-expressing plasmid, the one containing the target sequence no. 1, CATTGGTAATGTGATGAATAAA, was chosen for the study.

Immunofluorescence

Cells growing on coverslips in 12-well plates were left untreated or were transfected with different expression constructs. At 16 or 48 h after transfection, cells were washed in phosphate-buffered saline (PBS) and fixed for 5 min in methanol (−20°C). Cells were rehydrated in PBS and incubated with primary antibodies diluted in 0.5% goat serum (Sigma) in PBS for 16 h at 4°C. Cells were rinsed in PBS, then secondary antibodies were added for 1 h at room temperature. The following antibodies were used: immunopurified rabbit polyclonal anti-CDKL5 (1:5) (17), mouse monoclonal anti-SC35 (1:20, Sigma-Aldrich), mouse monoclonal anti-Sm (1:100, Thermo Scientific, Fremont, USA), mouse monoclonal anti-GFP (1:500, Invitrogen), rabbit polyclonal anti-GFP (1:500, Invitrogen). Alexa 488 and 594 anti-mouse and anti-rabbit IgG secondary antibodies (1:500, Molecular Probes) were used for detection. Coverslips were mounted onto slides in fluorescent mounting medium (DakoCytomation, Glostrup, Denmark) and analyzed with a Nikon Eclipse E600 fluorescent microscope (Nikon, Tokyo, Japan). Images were captured using a digital camera (DXM 1200, Nikon) with the ACT-1 software (Nikon).

Western blotting

NIH3T3 cells were plated in six-well plates, transfected with Lipofectamine Plus Reagent and harvested in ice-cold PBS. Cells were lysed in lysis buffer (Tris–HCl 50 mM pH 8.0, NaCl 150 mM, 1% NP-40, 0.1% SDS and a mix of phosphatases and proteases inhibitors from Sigma-Aldrich) for 15 min at 4°C. Lysates were clarified by centrifugation for 15 min at 18 000*g*, and protein concentration of the supernatant was determined using BSA as a standard (Bradford reagent assay, Sigma-Aldrich). Total lysates were boiled in SDS sample buffer, separated by SDS–PAGE and blotted to nitrocellulose membrane (Amersham). Filters were blocked in tris-buffered saline tween-20 (0.1%) (TBST) (10 mM Tris–HCl, pH 8.0, 150 mM NaCl and 0.05% Tween-20) plus 5% dried milk and incubated with primary antibodies for 16 h at 4°C. The following primary antibodies were used: rabbit polyclonal anti-CDKL5 (1:100), mouse monoclonal anti-ASF/SF2 (1:500), mouse monoclonal anti-Sm (1:100, Thermo Scientific), mouse monoclonal anti-Tubulin (1:1000, Sigma-Aldrich), mouse monoclonal anti-GFP (1:500, Roche Diagnostics, Basel, Switzerland), rabbit polyclonal anti-GFP (1:250, Invitrogen). After washing three times with TBST, filters were incubated with peroxidase-conjugated secondary antibodies (anti-mouse or rabbit Ig; 1:5000) (Amersham) for 1 h at room temperature. Detection was performed by enhanced chemiluminescence (EuroClone, Pero, Italy). For quantitative measurements, autoradiographs were scanned and signal intensity assessed with ImageJ (NIH) software.

Immunoprecipitation

For co-immunoprecipitation, NIH3T3 cells were grown on 100 mm Petri dishes and transiently transfected with calcium phosphate precipitation method. At 24 h after transfection, cells were collected, resuspended in lysis buffer (Tris–HCl 50 mM pH 8.0, NaCl 150 mM, 1% NP-40) supplemented with

protease and phophatase inhibitors (Sigma-Aldrich), and centrifuged for 15 min at 18 000*g* at 4°C. The extract was immunoprecipitated with 10 μl of anti-GFP monoclonal antibody (Roche-Diagnostics) for 16 h at 4°C; 50 μl of Protein G-agarose beads (Invitrogen) were then added and the immunoprecipitate was further incubated for 4 h at 4°C. Immunocomplexes were collected by centrifugation, washed three times with lysis buffer, separated on a 8% SDS–PAGE, blotted to nitrocellulose membrane (Amersham) and analyzed by western blot.

E1A splicing assay

NIH3T3 cells grown on six-well plates were co-transfected with 1 mg of E1A plasmid and 4 mg of either GFP-CDKL5-WT, GFP-CDKL5-K42R or GFP empty vector. At 24 h after transfection, cells were harvested and total RNA was with RNAeasy Micro Kit (Quiagen). Reverse transcription was carried out on 2 mg of total RNA, using oligo-dT and with Transcriptor High Fidelity cDNA Synthesis Kit (Roche). The E1A splice isoforms were detected by PCR using E1A primers (5′-TTTGGACCAGCTGATCGAAG-3′ and 5′-TAACCATTATAAGCTGCAAT-3′). Amplification was carried out for 23 cycles in a 25 ml volume with 2 ml of cDNA. PCR products were resolved on 1.5% agarose gel, visualized by ethidium bromide staining and quantitated by densitometric scanning.

Human primary skin fibroblasts

After informed consent from the parents, a skin biopsy was performed from the upper arm of the girl carrying the p.R59X CDKL5 mutation. A primary dermal fibroblast culture was concomitantly established. Fibroblasts were cultured in Dulbecco's modified Eagle's medium with glutaMAX, supplemented with 10% fetal calf serum (Gibco, Invitrogen, Cergy-Pontoise, France), penicillin (100 IU/ml) and streptomycin (100 μg/ml) (PAA Laboratories, Pasching, Austria) in a humidified atmosphere containing 5% CO_2 at 37°C. Passages two to five were used for the experiments.

SUPPLEMENTARY MATERIAL

Supplementary Material is available at *HMG* online.

ACKNOWLEDGEMENTS

We are grateful to Carlo Sala for advice on primary neuronal cultures and providing primary antibodies, David Spector for YFP-SC35, Davide Gabellini and Valeria Marigo for ASF/SF2 and SC35 antibodies, respectively. Stefano Biffo, Stefano Grosso and all members of the Broccoli's laboratory are acknowledged for valuable discussion.

Conflict of Interest statement. None declared.

FUNDING

This work was supported by the International Rett Syndrome Foundation (IRSF) (B.V.), the E-Rare EuroRETT Network (B.V. and L.N.), the Italian Ministry of Research (K.N.C. and B.V.), the Telethon Foundation (L.N. and B.V.) and the Cariplo Foundation (L.N.).

REFERENCES

1. Bienvenu, T. and Chelly, J. (2006) Molecular genetics of Rett syndrome: when DNA methylation goes unrecognized. *Nat. Rev. Genet.*, **7**, 415–426.
2. Weaving, L.S., Ellaway, C.J., Gécz, J. and Christodoulou, J. (2005) Rett syndrome: clinical review and genetic update. *J. Med. Genet.*, **42**, 1–7.
3. Kalscheuer, V.M., Tao, J., Donnelly, A., Hollway, G., Schwinger, E., Kübart, S., Menzel, C., Hoeltzenbein, M., Tommerup, N., Eyre, H. *et al.* (2003) Disruption of the serine/threonine kinase 9 gene causes severe X-linked infantile spasms and mental retardation. *Am. J. Hum. Genet.*, **72**, 1401–1411.
4. Tao, J., Van Esch, H., Hagedorn-Greiwe, M., Hoffmann, K., Moser, B., Raynaud, M., Sperner, J., Fryns, J.P., Schwinger, E., Gécz, J. *et al.* (2004) Mutations in the X-linked cyclin-dependent kinase-like 5 (CDKL5/STK9) gene are associated with severe neurodevelopmental retardation. *Am. J. Hum. Genet.*, **75**, 1149–1154.
5. Weaving, L.S., Christodoulou, J., Williamson, S.L., Friend, K.L., McKenzie, O.L., Archer, H., Evans, J., Clarke, A., Pelka, G.J., Tam, P.P. *et al.* (2004) Mutations of CDKL5 cause a severe neurodevelopmental disorder with infantile spasms and mental retardation. *Am. J. Hum. Genet.*, **75**, 1079–1093.
6. Archer, H.L., Evans, J., Edwards, S., Colley, J., Newbury-Ecob, R., O'Callaghan, F., Huyton, M., O'Regan, M., Tolmie, J., Sampson, J. *et al.* (2006) CDKL5 mutations cause infantile spasms, early onset seizures, and severe mental retardation in female patients. *J. Med. Genet.*, **43**, 729–734.
7. Rosas-Vargas, H., Bahi-Buisson, N., Philippe, C., Nectoux, J., Girard, B., N'Guyen Morel, M.A., Gitiaux, C., Lazaro, L., Odent, S., Jonveaux, P. *et al.* (2008) Impairment of CDKL5 nuclear localisation as a cause for severe infantile encephalopathy. *J. Med. Genet.*, **45**, 172–178.
8. Bahi-Buisson, N., Nectoux, J., Rosas-Vargas, H., Milh, M., Boddaert, N., Girard, B., Cances, C., Ville, D., Afenjar, A., Rio, M. *et al.* (2008) Key clinical features to identify girls with CDKL5 mutations. *Brain*, **131**, 2647–2661.
9. Artuso, R., Mencarelli, M.A., Polli, R., Sartori, S., Ariani, F., Pollazzon, M., Marozza, A., Cilio, M.R., Specchio, N., Vigevano, F. *et al.* (2009) Early-onset seizure variant of Rett syndrome: definition of the clinical diagnostic criteria. *Brain Dev.*, [Epub ahead of print].
10. Russo, S., Marchi, M., Cogliati, F., Bonati, M.T., Pintaudi, M., Veneselli, E., Saletti, V., Balestrini, M., Ben-Zeev, B. and Larizza, L. (2009) Novel mutations in the CDKL5 gene, predicted effects and associated phenotypes. *Neurogenetics*, [Epub ahead of print].
11. Scala, E., Ariani, F., Mari, F., Caselli, R., Pescucci, C., Longo, I., Meloni, I., Giachino, D., Bruttini, M., Hayek, G. *et al.* (2005) CDKL5/STK9 is mutated in Rett syndrome variant with infantile spasms. *J. Med. Genet.*, **42**, 103–107.
12. Mari, F., Azimonti, S., Bertani, I., Bolognese, F., Colombo, E., Caselli, R., Scala, E., Longo, I., Grosso, S., Pescucci, C. *et al.* (2005) CDKL5 belongs to the same molecular pathway of MeCP2 and it is responsible for the early-onset seizure variant of Rett syndrome. *Hum. Mol. Genet.*, **14**, 1935–1946.
13. Evans, J.C., Archer, H.L., Colley, J.P., Ravn, K., Nielsen, J.B., Kerr, A., Williams, E., Christodoulou, J., Gécz, J., Jardine, P.E. *et al.* (2005) Early onset seizures and Rett-like features associated with mutations in CDKL5. *Eur. J. Hum. Genet.*, **13**, 1113–1120.
14. Chahrour, M. and Zoghbi, H.Y. (2007) The story of Rett syndrome: from clinic to neurobiology. *Neuron*, **56**, 422–437.
15. Van Esch, H., Jansen, A., Bauters, M., Froyen, G. and Fryns, J.P. (2007) Encephalopathy and bilateral cataract in a boy with an interstitial deletion of Xp22 comprising the CDKL5 and NHS genes. *Am. J. Med. Genet. A*, **143**, 364–369.
16. Elia, M., Falco, M., Ferri, R., Spalletta, A., Bottitta, M., Calabrese, G., Carotenuto, M., Musumeci, S.A., Lo Giudice, M. and Fichera, M. (2008) CDKL5 mutations in boys with severe encephalopathy and early-onset intractable epilepsy. *Neurology*, **71**, 997–999.
17. Rusconi, L., Salvatoni, L., Giudici, L., Bertani, I., Kilstrup-Nielsen, C., Broccoli, V. and Landsberger, N. (2008) CDKL5 expression is modulated

during neuronal development and its subcellular distribution is tightly regulated by the C-terminal tail. *J. Biol. Chem.*, **283**, 30101–30111.
18. Lin, C., Franco, B. and Rosner, M.R. (2005) CDKL5/Stk9 kinase inactivation is associated with neuronal developmental disorders. *Hum. Mol. Genet.*, **14**, 3775–3786.
19. Kameshita, I., Sekiguchi, M., Hamasaki, D., Sugiyama, Y., Hatano, N., Suetake, I., Tajima, S. and Sueyoshi, N. (2008) Cyclin-dependent kinase-like 5 binds and phosphorylates DNA methyltransferase 1. *Biochem. Biophys. Res. Commun.*, **377**, 1162–1167.
20. Bertani, I., Rusconi, L., Bolognese, F., Forlani, G., Conca, B., De Monte, L., Badaracco, G., Landsberger, N. and Kilstrup-Nielsen, C. (2006) Functional consequences of mutations in CDKL5, an X-linked gene involved in infantile spasms and mental retardation. *J. Biol. Chem.*, **281**, 32048–32056.
21. Lamond, A.I. and Spector, D.L. (2003) Nuclear speckles: a model for nuclear organelles. *Nat. Rev. Mol. Cell Biol.*, **4**, 605–612.
22. Handwerger, K.E. and Gall, J.G. (2005) Subnuclear organelles: new insights into form and function. *Trends Cell Biol.*, **16**, 19–26.
23. Hall, L.L., Smith, K.P., Byron, M. and Lawrence, J.B. (2006) Molecular anatomy of a speckle. *Anat. Rec. A Discov. Mol. Cell Evol. Biol.*, **288**, 664–675.
24. Gui, J.F., Lane, W.S. and Fu, X.D. (1994) A serine kinase regulates intracellular localization of splicing factors in the cell cycle. *Nature*, **369**, 678–682.
25. Colwill, K., Pawson, T., Andrews, B., Prasad, J., Manley, J.L., Bell, J.C. and Duncan, P.I. (1996) The Clk/Sty protein kinase phosphorylates SR splicing factors and regulates their intranuclear distribution. *EMBO J.*, **15**, 265–275.
26. Mermoud, J.E., Cohen, P.T. and Lamond, A.I. (1994) Regulation of mammalian spliceosome assembly by a protein phosphorylation mechanism. *EMBO J.*, **13**, 5679–5688.
27. Misteli, T., Cáceres, J.F., Clement, J.Q., Krainer, A.R., Wilkinson, M.F. and Spector, D.L. (1998) Serine phosphorylation of SR proteins is required for their recruitment to sites of transcription in vivo. *J. Cell Biol.*, **143**, 297–307.
28. Wahl, M., Will, C.L. and Lührmann, R. (2009) The spliceosome: design principles of a dynamic RNP machine. *Cell*, **136**, 701–718.
29. Zhong, X.Y., Ding, J.H., Adams, J.A., Ghosh, G. and Fu, X.D. (2009) Regulation of SR protein phosphorylation and alternative splicing by modulating kinetic interactions of SRPK1 with molecular chaperones. *Genes Dev.*, **23**, 482–495.
30. Long, J.C. and Cáceres, J.F. (2009) The SR protein family of splicing factors: master regulators of gene expression. *Biochem. J.*, **417**, 15–27.
31. Solis, A.S., Peng, R., Crawford, J.B., Phillips, J.A. III and Patton, J.G. (2008) Growth hormone deficiency and splicing fidelity: two serine/arginine-rich proteins, ASF/SF2 and SC35, act antagonistically. *J. Biol. Chem.*, **283**, 23619–23626.
32. Cáceres, J.F., Stamm, S., Helfman, D.M. and Krainer, A.R. (1994) Regulation of alternative splicing *in vivo* by overexpression of antagonistic splicing factors. *Science*, **265**, 1706–1709.
33. Wang, P., Lou, P.J., Leu, S. and Ouyang, P. (2002) Modulation of alternative pre-mRNA splicing *in vivo* by pinin. *Biochem. Biophys. Res. Commun.*, **294**, 448–455.
34. Yomoda, J., Muraki, M., Kataoka, N., Hosoya, T., Suzuki, M., Hagiwara, M. and Kimura, H. (2008) Combination of Clk family kinase and SRp75 modulates alternative splicing of Adenovirus E1A. *Genes Cells*, **13**, 233–244.
35. Manley, J.L. and Tacke, R. (1996) SR proteins and splicing control. *Genes Dev.*, **10**, 1569–1579.
36. Misteli, T. and Spector, D.L. (1997) Protein phosphorylation and the nuclear organization of pre-mRNA splicing. *Trends Cell Biol.*, **7**, 135–138.
37. Cáceres, J.F. and Kornblihtt, A.R. (2002) Alternative splicing: multiple control mechanisms and involvement in human disease. *Trends Genet.*, **18**, 186–193.
38. Prasad, J., Colwill, K., Pawson, T. and Manley, J.L. (1999) The protein kinase Clk/Sty directly modulates SR protein activity: both hyper- and hypophosphorylation inhibit splicing. *Mol. Cell Biol.*, **19**, 6991–7000.
39. Comitato, A., Spampanato, C., Chakarova, C., Sanges, D., Bhattacharya, S.S. and Marigo, V. (2007) Mutations in splicing factor PRPF3, causing retinal degeneration, form detrimental aggregates in photoreceptor cells. *Hum. Mol. Genet.*, **16**, 1699–1707.
40. Cooper, T.A., Wan, L. and Dreyfuss, G. (2009) RNA and disease. *Cell*, **136**, 777–793.
41. Buratti, E. and Baralle, F.E. (2008) Multiple roles of TDP-43 in gene expression, splicing regulation, and human disease. *Front. Biosci.*, **13**, 867–878.
42. Battle, D.J., Kasim, M., Yong, J., Lotti, F., Lau, C.K., Mouaikel, J., Zhang, Z., Han, K., Wan, L. and Dreyfuss, G. (2006) The SMN complex: an assembly machine for RNPs. *Cold Spring Harb. Symp. Quant. Biol.*, **71**, 313–320.
43. Zhang, Z., Lotti, F., Dittmar, K., Younis, I., Wan, L., Kasim, M. and Dreyfuss, G. SMN deficiency causes tissue-specific perturbations in the repertoire of snRNAs and widespread defects in splicing. *Cell*, **133**, 585–600.
44. Chahrour, M. and Zoghbi, H.Y. The story of Rett syndrome: from clinic to neurobiology. *Neuron*, **56**, 422–437.
45. Young, J.I., Hong, E.P., Castle, J.C., Crespo-Barreto, J., Bowman, A.B., Rose, M.F., Kang, D., Richman, R., Johnson, J.M., Berget, S. *et al.* (2005) Regulation of RNA splicing by the methylation-dependent transcriptional repressor methyl-CpG binding protein 2. *Proc. Natl Acad. Sci. USA*, **102**, 17551–17558.